Figures and figure supplements

Cell-autonomous role of leucine-rich repeat kinase in the protection of dopaminergic neuron survival

Jongkyun Kang and Guodong Huang *et al*.

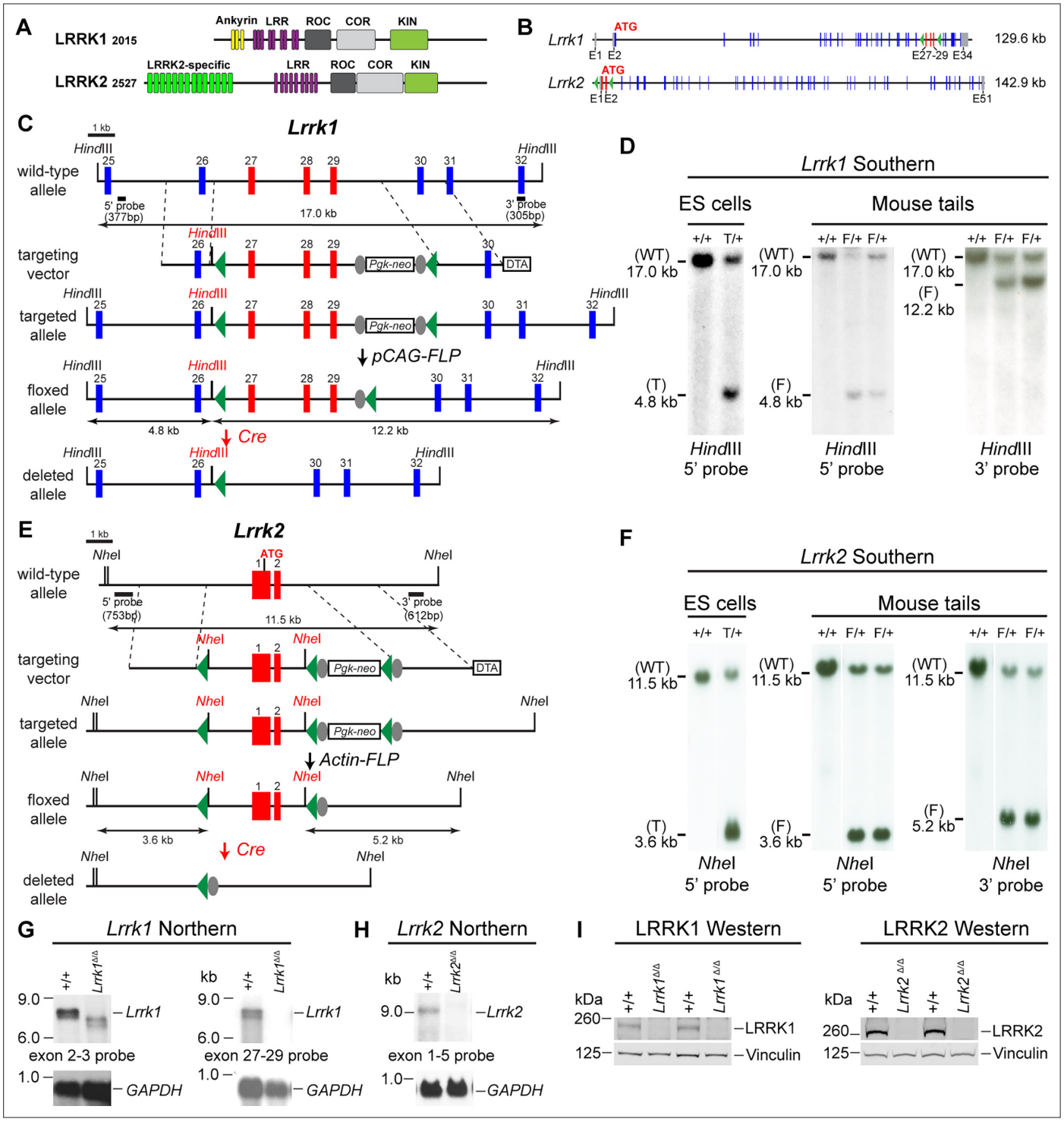

Figure 1. Generation and characterization of floxed and deleted *Lrrk1* and *Lrrk2* alleles. (**A**) Schematic illustrations of human LRRK1 and LRRK2 proteins showing similar functional domains. $LRRK1_{2015}$ protein is derived from exons 2–34 (Ensembl Genome Database: ENSG00000154237). $LRRK2_{2527}$ protein is derived from exons 1–51 (ENSG00000188906). LRR: leucine-rich repeats; Roc: Ras-of-complex; COR: C-terminal of Roc; KIN: kinase domain. (**B**) Schematic illustrations of the gene structures of mouse *Lrrk1* and *Lrrk2*. The boxes in blue are exons that encode the LRRK1 and LRRK2 proteins, and the gray boxes represent the 5' and 3' UTRs. The exons are not drawn in scale. The start codon ATG is in exon 2 of *Lrrk1* and exon 1 of *Lrrk2*. The exons 27–29 of *Lrrk1* and the promoter/exons 1–2 of *Lrrk2* are flanked with loxP sites (green arrowheads). (**C**) Targeting strategy for the generation of the targeted, floxed, and deleted *Lrrk1* alleles. The red boxes represent the targeted exons 27–29, and the blue boxes represent the untargeted exons. The locations and sizes of the 5' and 3' external probes are shown. The targeting vector contains the 5' and 3' homologous regions (marked by dashed lines) and the middle region (from intron 26 to intron 29), which includes a loxP site (green arrowhead) in intron 26 (1288 bp upstream of exon

Figure 1 continued on next page

Figure 1 continued

27) and the *Pgk-neo* selection cassette flanked by two FRT (FLP recognition target) sequences (gray circles) followed by another loxP site in intron 29 (1023 bp downstream of exon 29). A negative selection cassette encoding diphtheria toxin fragment A (DTA) is also included in the targeting vector to reduce embryonic stem (ES) cells bearing randomly inserted targeting vectors. ES cells carrying the correctly targeted *Lrrk1* allele were transfected with *pCAG-FLP* to remove the *Pgk-neo* cassette and generate the floxed *Lrrk1* allele. Floxed *Lrrk1* mice were bred with *CMV-Cre* transgenic mice to generate germline deleted *Lrrk1* mice. Detailed strategy for generating targeting vector and DNA sequence of floxed *Lrrk1* allele can be found in ***Figure 1—figure supplement 1*** and ***Supplementary file 1***, respectively. (**D**) Southern analysis of the targeted and floxed *Lrrk1* alleles. Genomic DNA from ES cells or mouse tails was digested with *Hind*III and hybridized with the 5' or 3' external probe. For the 5' probe, the resulting 17.0 kb and 4.8 kb bands represent the wild-type (WT) and the targeted (T) or floxed (F) alleles, respectively. For the 3' probe, the resulting 17.0 kb and 12.2 kb bands represent the WT and the floxed alleles, respectively. Detailed Southern strategy can be found in ***Figure 1—figure supplement 2***. (**E**) Targeting strategy for the generation of the targeted, floxed, and deleted *Lrrk2* alleles. The red boxes represent *Lrrk2* exons 1 and 2, and the start codon ATG resides in exon 1. The locations and sizes of the 5' and 3' external probes are shown. The targeting vector contains the 5' and 3' homologous regions (marked by dashed lines) and the middle region (from the promoter to intron 2), which includes a loxP site (green arrowhead) upstream (1768 bp) of the transcription initiation site and the *Pgk-neo* selection cassette flanked by two FRT sequences (gray circles) and two loxP sites (green arrowheads) in intron 2 (878 bp downstream of exon 2). A negative selection cassette encoding DTA is also included in the targeting vector. Mice carrying the correctly targeted *Lrrk2* allele were crossed with *Actin-FLP* deleter mice to generate floxed *Lrrk2* mice, which were bred with *CMV-Cre* transgenic mice to generate germline deleted *Lrrk2* mice. Detailed strategy for generating targeting vector and the DNA sequence of the floxed *Lrrk2* allele can be found in ***Figure 1—figure supplement 3***, respectively. (**F**) Southern analysis of the targeted and floxed *Lrrk2* alleles. Genomic DNA from ES cells or mouse tails was digested with *Nhe*I and hybridized with the 5' or 3' external probe. For the 5' probe, the resulting 11.5 kb and 3.6 kb bands represent the wild-type (WT) and the targeted (T) or floxed (F) alleles, respectively. For the 3' probe, the resulting 11.5 kb and 5.2 kb bands represent the WT and the floxed *Lrrk2* alleles, respectively. Detailed Southern strategy can be found in ***Figure 1—figure supplement 4***. (**G**) Northern analysis of poly(A)+RNA prepared from the lung of $Lrrk1^{\Delta/\Delta}$ mice carrying homozygous germline deleted (Δ/Δ) *Lrrk1* alleles derived from $Lrrk1^{F/F}$ mice using the cDNA probe of exons 2–3 (left) and exons 27–29 (right). Using the upstream exons 2–3 probe, the *Lrrk1* transcripts in wild-type mice are the expected size of ~7.4 kb, whereas the detected *Lrrk1* transcripts in $Lrrk1^{\Delta/\Delta}$ mice are truncated, consistent with the deletion of exons 27–29 (625 bp), which results in a frameshift, and are expressed at lower levels, likely due to nonsense-mediated degradation of the truncated *Lrrk1* mRNA. Using a probe specific for exons 27–29, there is no *Lrrk1* transcript in $Lrrk1^{\Delta/\Delta}$ mice, as expected. Both blots were hybridized with a *GAPDH* probe as loading controls. Detailed northern strategy and full-size blots are included in ***Figure 1—figure supplements 5 and 6***, respectively. Extensive RT-PCR analysis of *Lrrk1* transcripts in $Lrrk1^{\Delta/\Delta}$ mice is shown in ***Figure 1—figure supplement 7***. (**H**) Northern analysis of total RNA prepared from the neocortex of $Lrrk2^{\Delta/\Delta}$ mice carrying homozygous germline *Lrrk2* deleted (Δ/Δ) alleles using the cDNA probe of exons 1–5 shows the absence of *Lrrk2* transcripts. The blot was hybridized with a *GAPDH* probe as a loading control. The full-size blot is included in ***Figure 1—figure supplement 8***. RT-PCR analysis of *Lrrk2* transcripts in $Lrrk2^{\Delta/\Delta}$ mice is shown in ***Figure 1—figure supplement 9***. (**I**) Left: western analysis of wild-type (+/+) and homozygous $Lrrk1^{\Delta/\Delta}$ (Δ/Δ) brains shows the absence of LRRK1 protein. Right: western analysis of the neocortex of wild-type (+/+) and homozygous $Lrrk2^{\Delta/\Delta}$ (Δ/Δ) mice shows the absence of LRRK2 protein. Vinculin was used as a loading control. Full-size blots can be found in ***Figure 1—source data 1***.

Figure 1—figure supplement 1. Genomic DNA sequence of the floxed *Lrrk1* allele.

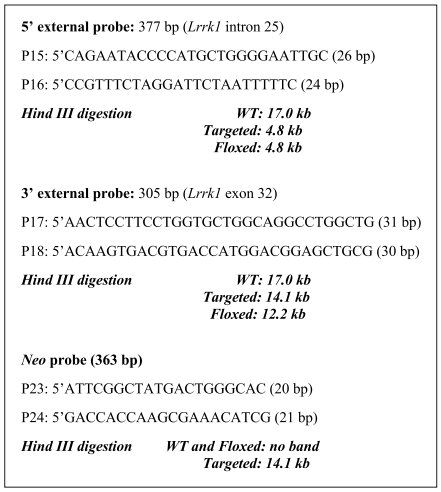

Figure 1—figure supplement 2. Southern strategy for the targeted and floxed *Lrrk1* alleles.

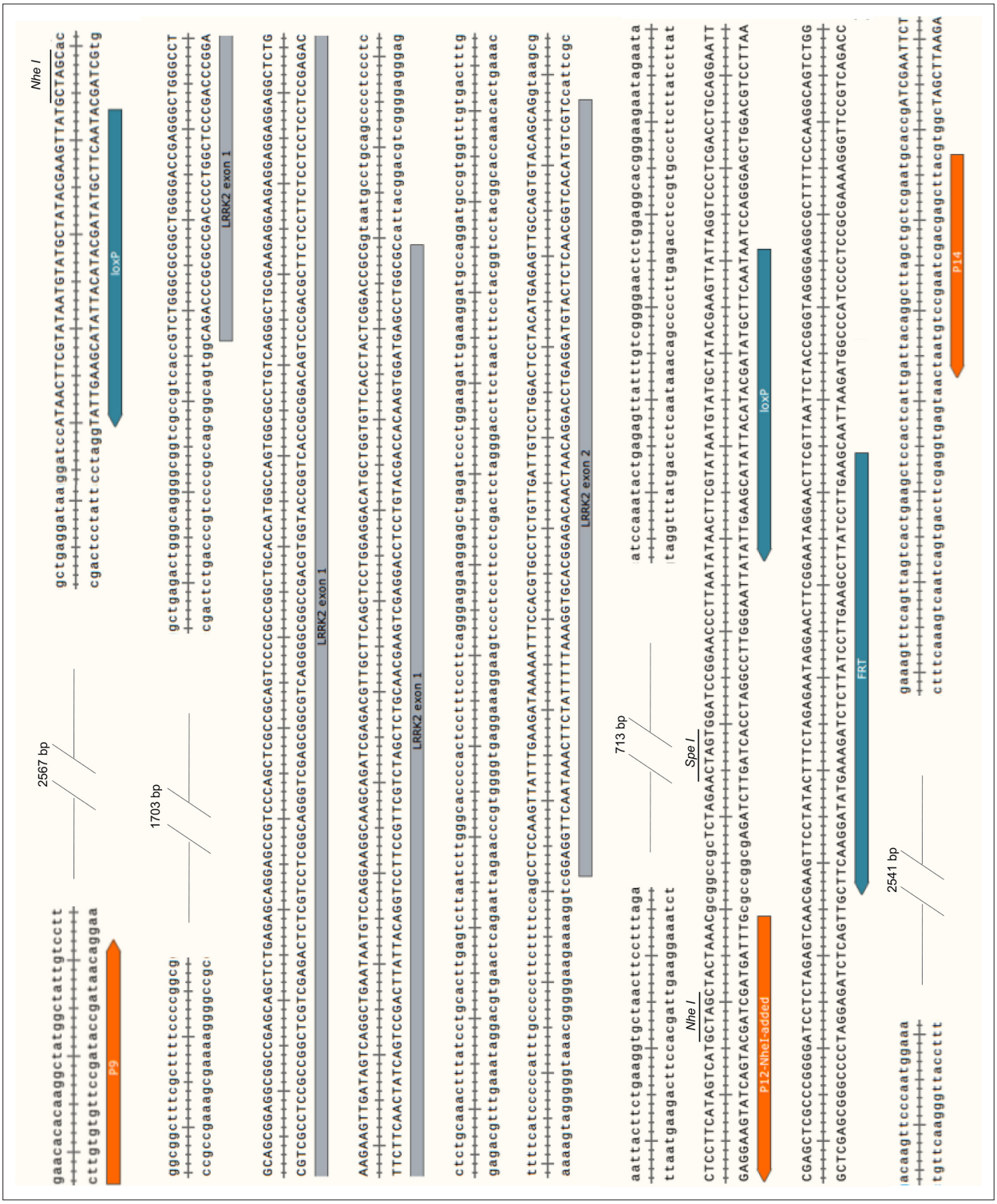

Figure 1—figure supplement 3. Genomic DNA sequence of the floxed *Lrrk2* allele.

5' external probe (753 bp)

P19= 5'CATGGGAGAGAGGGTTTCTCACTTACT (27 bp)

P20= 5'CTTGGACAGCATTGTCAGCCTAGAC (25 bp)

Nhe I digestion ***WT: 11.5 kb***
Targeted and floxed: 3.6 kb

3' external probe (622 bp)

P21=5' GCCAAGCAGTTATTGATGCTGTAGC (31 bp)

P22= 5' CGAGCTGTAAGATGAGCTGGGTACT (30 bp)

Sph I digestion ***WT: 12.3 kb***
Targeted: 4.5 kb

Nhe I digestion ***WT: 11.5 kb***
Floxed: 5.2 kb

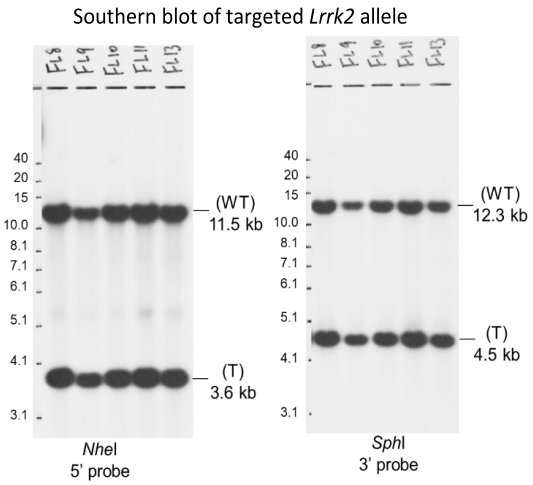

Figure 1—figure supplement 4. Southern analysis of the targeted and floxed *Lrrk2* alleles.

***Lrrk1* exons 2-3 probe (377+4=383 bp)**

P31: 5' CAGGATGAGCGTGTGTCTGCAG (CAG exon 1/rest exon2)

P32: 5′ CCTTCTCCTGTGAGGATTCGCTCT (C exon 3/rest exon 4)

WT and floxed alleles: ~7.4 kb

Deleted allele: ~6.8 kb*

* Deletion of *Lrrk1* exons 27-29 (625 bp; exon 27: 278 bp, exon 28: 195 bp, exon 29 152 bp) results in frameshift of downstream exons, likely resulting in degradation of the transcript.

***Lrrk1* exons 27-29 probe (550 bp)**

P33: 5' CTGGCCTACCTGCACAAGAA (exon 27)

P34: 5' CCTTCCCATCCCAGAACACC (exon 29)

WT and floxed alleles: 7.4 kb

Deleted allele: no band

***GAPDH* probe (452 bp)**

P37: 5' ACCACAGTCCATGCCATCAC (exon 5)

P38: 5′ TCCACCACCCTGTTGCTGTA (exon 7)

Figure 1—figure supplement 5. Northern strategy for *Lrrk1* mRNA.

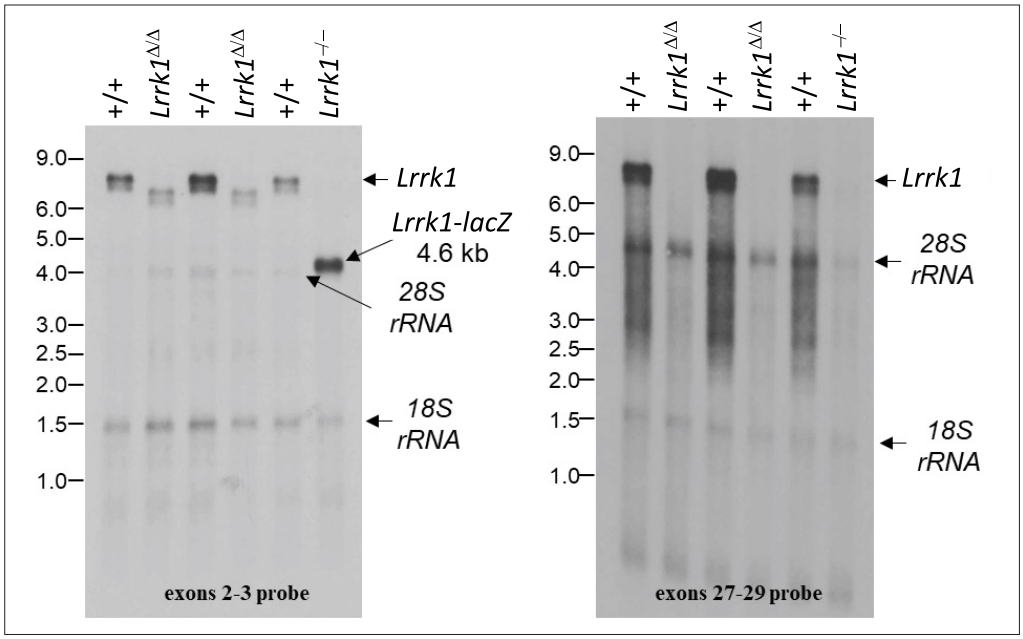

Figure 1—figure supplement 6. Northern analysis of *Lrrk1* mRNA in *Lrrk1*$^{\Delta/\Delta}$ mice.

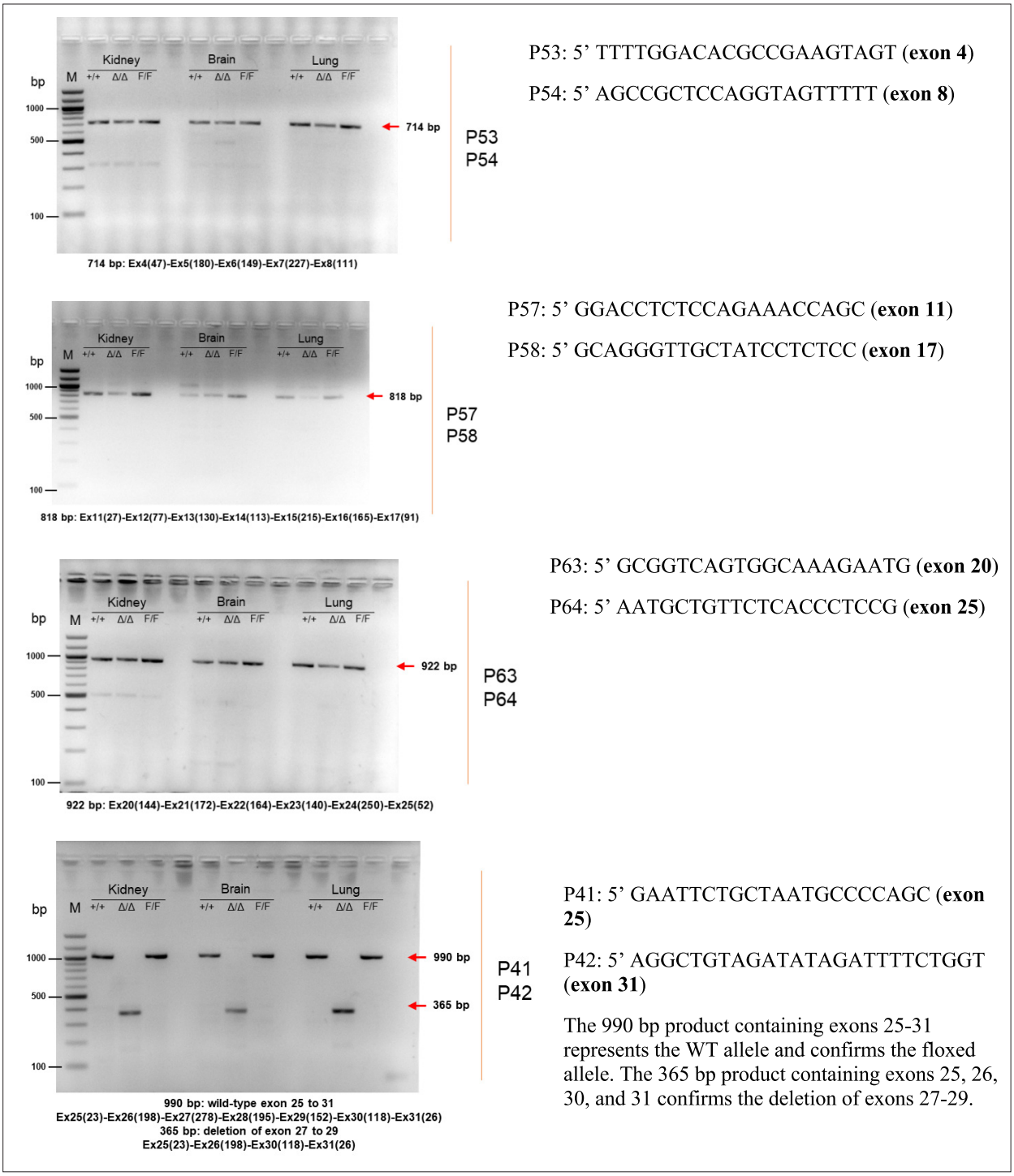

Figure 1—figure supplement 7. RT-PCR analysis of the deleted *Lrrk1* allele.

***Lrrk2* exons 1-5 probe (437 bp)**

P35= 5' AGGAAGGCAAGCAGATCGAG (exon 1, 20 bp)

P20= 5' GGCTGAATATCTGTGCATGGC (exon 5, 22 bp)

WT and floxed alleles: 8.3 kb
Deletion: no band

***GAPDH* probe (452 bp)**

P37= 5' ACCACAGTCCATGCCATCAC (exon 5, 20 bp)

P38= 5′ TCCACCACCCTGTTGCTGTA (exon 7, 20 bp)

Lrrk2 Northern blot (total RNA from the brain) using exons 1-5 probe: The probe detected the full-length *Lrrk2* transcript (~8.3 kb) in wild-type (+/+) and $Lrrk2^{F/F}$ mice, and no transcript in $LRRK2^{\Delta/\Delta}$ mice, derived from floxed *LRRK2* alleles, and previously generated $LRRK^{-/-}$ mice (Giaime et al., *Neuron*, 2017).

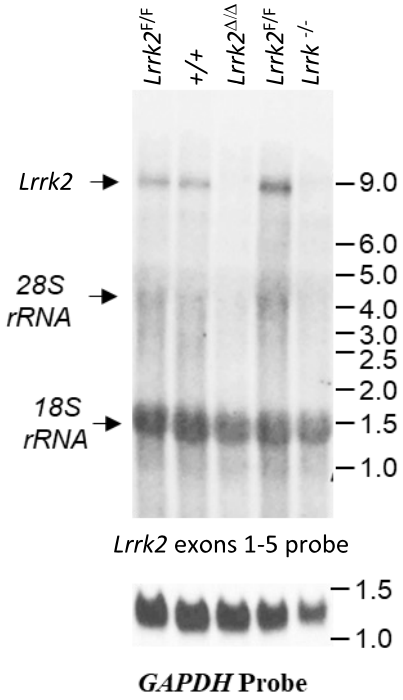

Figure 1—figure supplement 8. Northern analysis of *Lrrk2* mRNA in $Lrrk2^{F/F}$ and $Lrrk2^{\Delta/\Delta}$ mice.

RT-PCR analysis using an *Lrrk2* exon 51-specific primer P93 (5'TCGTGTGGAAGATTGAGGTCC) for RT, and primers in *Lrrk2* exons 1 and 5, P35 and P20, for PCR, which shows normal splicing in $Lrrk2^{F/F}$ (F/F) brains and the absence of PCR products in $Lrrk2^{\Delta/\Delta}$ (Δ/Δ) brains. The identity of the PCR product in +/+ and $Lrrk2^{F/F}$ (F/F) brains was confirmed by sequencing: The 437 bp product contains *Lrrk2* exons 1-5.

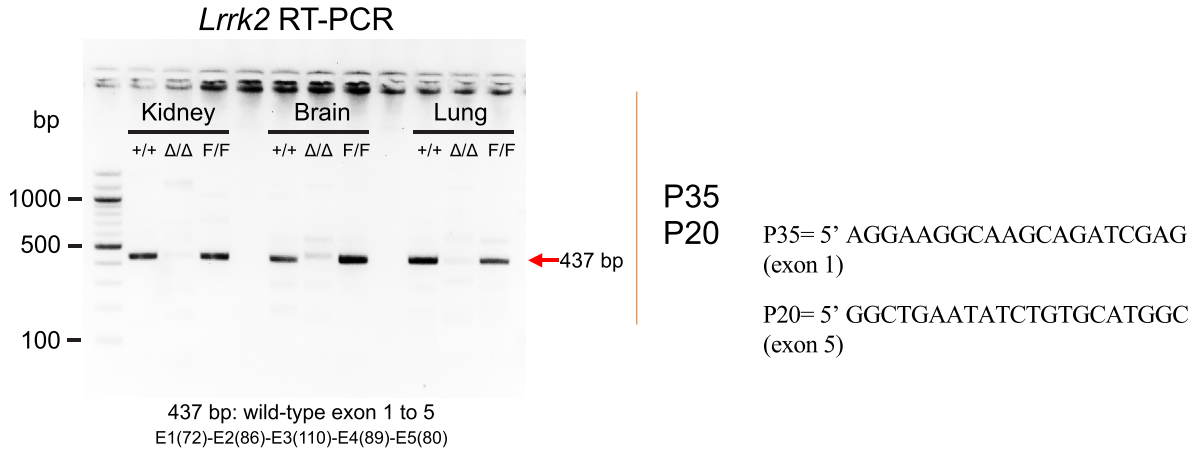

Figure 1—figure supplement 9. RT-PCR analysis of the deleted *Lrrk2* allele.

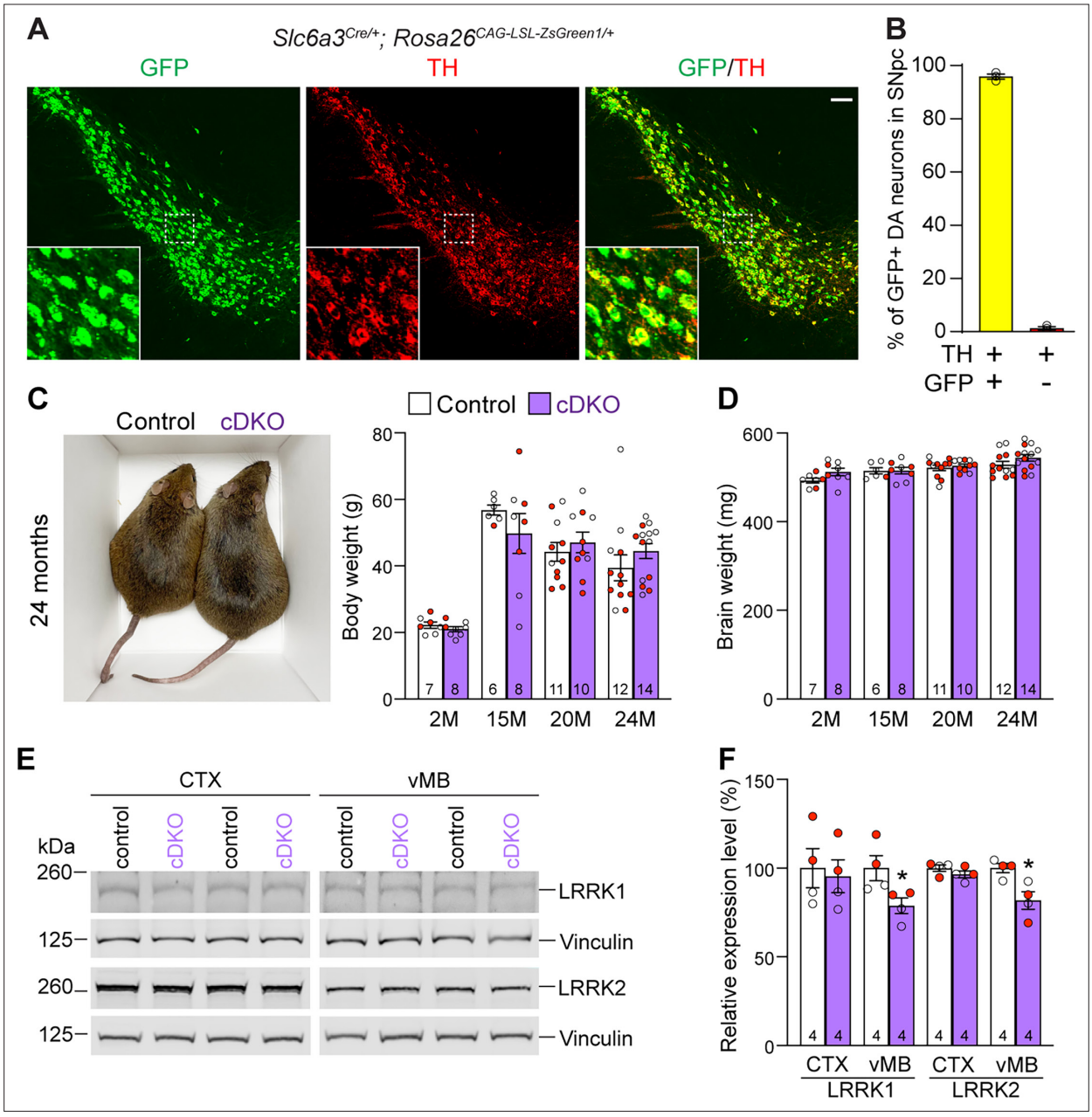

Figure 2. Generation and characterization of dopaminergic (DA) neuron-specific *Lrrk* conditional double knockout (cDKO) mice. (**A**) Immunostaining of GFP and/or TH in the SNpc of *Slc6a3*$^{Cre/+}$; *Rosa26*$^{CAG\text{-}LSL\text{-}ZsGreen1/+}$ mice at 2 months of age. Cre recombinase is expressed under the control of the *Slc6a3* endogenous promoter and removes the floxed 'stop' cassette, resulting in the expression of EGFP under the control of the ubiquitous *CAG* promoter. (**B**) Quantification of GFP+/TH+ and TH+ cells shows that 99% of TH+ DA neurons (722 ± 46 TH+ cells) in the SNpc are also GFP+ (713 ± 46 cells), indicating that *Slc6a3-Cre* mediated recombination occurs in essentially all TH+ DA neurons. N = 3 mice, three comparable sections per hemisphere, 320 µm apart. (**C**) Similar body weight between *Lrrk* cDKO mice and littermate controls at all ages examined ($F_{1,68}$ = 0.001310, p=0.9712; 2M, 20M: p>0.9999; 15M: p=0.7857, 25M: p=0.8084, two-way ANOVA with Bonferroni's post hoc multiple comparisons). (**D**) Similar brain weight between *Lrrk* cDKO and control mice ($F_{1,68}$ = 3.603, p=0.0619; 2M: p=0.3893; 15M: p>0.9999; 20M: p>0.9999; 25M: p=0.3223, two-way ANOVA with Bonferroni's post hoc multiple comparisons). (**E**) Western analysis of LRRK1 and LRRK2 proteins in the dissected cerebral cortex (CTX) and ventral midbrain (vMB) of *Lrrk* cDKO and littermate controls at 2 months of age. (**F**) Quantification shows significant decreases in LRRK1 and LRRK2 in the dissected ventral midbrain of *Lrrk* cDKO mice (LRRK1, p=0.0432; LRRK2, p=0.0162, Student's *t*-test), compared to controls, but not in the dissected cortex of cDKO mice (LRRK1: p=0.7648; LRRK2: p=0.2325). The number in the column indicates the number of mice used in the study. Red-filled and open circles represent data obtained from individual male and female mice, respectively. All data are expressed as mean ± SEM. *p<0.05. Scale bar: 100 µm.

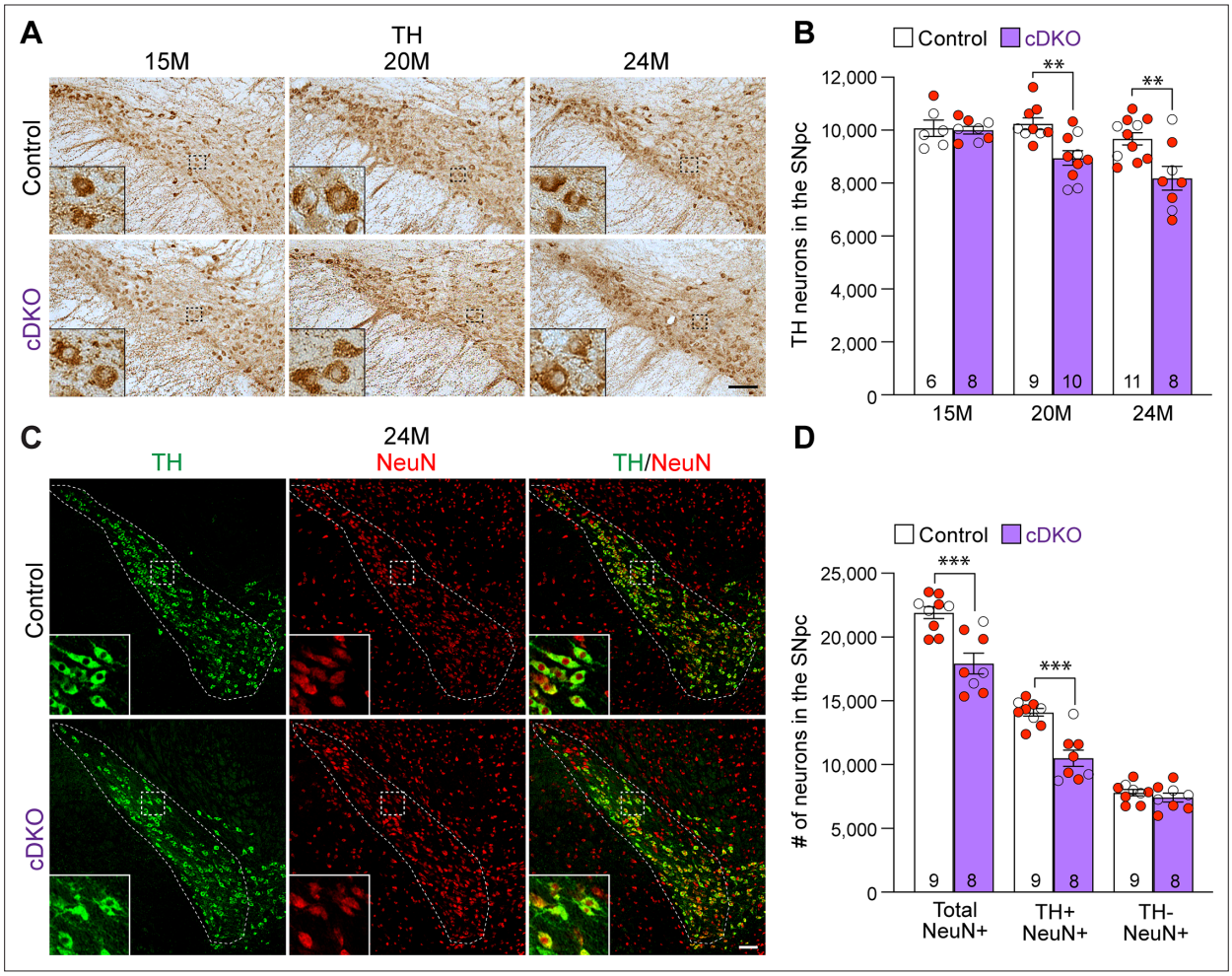

Figure 3. Age-dependent loss of dopaminergic (DA) neurons in the substantia nigra pars compacta (SNpc) of *Lrrk* conditional double knockout (cDKO) mice. (**A**) TH immunostaining shows TH+ DA neurons in the SNpc of *Lrrk* cDKO and littermate controls at the age of 15, 20, and 24 months. Higher power views of the boxed areas show grossly normal DA neuron morphology in *Lrrk* cDKO mice. (**B**) Quantification of TH+ DA neurons in the SNpc reveals similar numbers of DA neurons in *Lrrk* cDKO mice (10,000 ± 141) and littermate controls (10,077 ± 310, p>0.9999) at 15 months of age. At 20 months of age, the number of DA neurons in the SNpc of *Lrrk* cDKO mice (8948 ± 273) is significantly reduced compared to control mice (10,244 ± 220, $F_{1,46}$ = 16.59, p=0.0002; p=0.0041, two-way ANOVA with Bonferroni's post hoc multiple comparisons). By 24 months of age, the reduction of DA neurons in the SNpc of *Lrrk* cDKO mice (8188 ± 452) relative to controls (9675 ± 232, p=0.0010) is greater compared to 20 months of age. Raw quantification data are included in ***Figure 3—source data 1***. (**C**) Immunohistological analysis of TH and NeuN shows TH+ DA neurons (green) and NeuN+ neurons (red) in the SNpc of *Lrrk* cDKO mice and controls at 24 months of age. (**D**) Quantification of NeuN+ cells in the SNpc shows that the number of NeuN+ neurons in *Lrrk* cDKO mice (17,923 ± 813) is significantly lower than that in control mice (21,907 ± 469, p=0.0006, Student's *t*-test), indicating loss of neurons in the SNpc of *Lrrk* cDKO mice. All TH+ cells are NeuN+. The number of TH+/NeuN+ cells in the SNpc of *Lrrk* cDKO mice (10,500 ± 644) is also lower compared to control mice (14,102 ± 310, p=0.0001). There is no significant difference in the number of NeuN+/TH- neurons between littermate controls (7804 ± 249) and cDKO mice (7423 ± 344, p=0.3747). The number in the column indicates the number of mice used in the study. Red-filled and open circles represent data obtained from individual male and female mice, respectively. All data are expressed as mean ± SEM. **p<0.01, ***p<0.001. Scale bar: 100 μm.

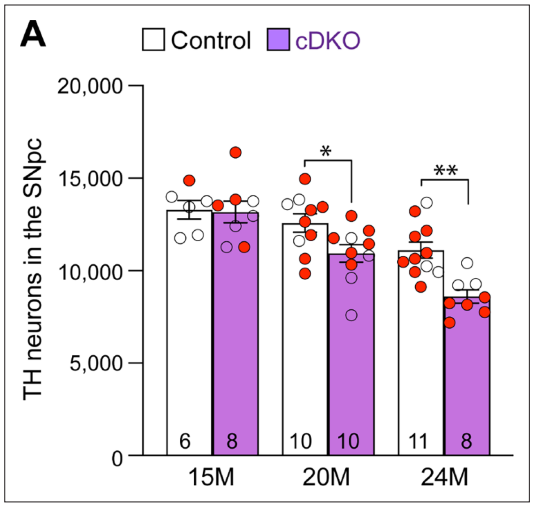

Figure 3—figure supplement 1. Independent validation of age-dependent reduction of dopaminergic (DA) neurons in the substantia nigra pars compacta (SNpc) of *Lrrk* conditional double knockout (cDKO) mice. (**A**) Quantification of TH+ DA neurons in the SNpc by an independent investigator using stereological methods sampling 25% areas of the SNpc. There are similar numbers of DA neurons in *Lrrk* cDKO mice (13,180 ± 585) and littermate controls (13,293 ± 500, p>0.9999) at 15 months of age. At 20 months of age, the number of DA neurons in the SNpc of *Lrrk* cDKO mice (10,936 ± 477) is significantly reduced compared to control mice (12,576 ± 497, $F_{1,47}$=12.40, p=0.0003; p=0.0423, two-way ANOVA with Bonferroni's post hoc multiple comparisons). By 24 months of age, the reduction of DA neurons in the SNpc of *Lrrk* cDKO mice (8600 ± 355) is more severe compared to controls (11,105 ± 435, p=0.0015). The number in the column indicates the number of mice used in the study. Red-filled and open circles represent data obtained from individual male and female mice, respectively. All data are expressed as mean ± SEM. *p<0.05, **p<0.01.

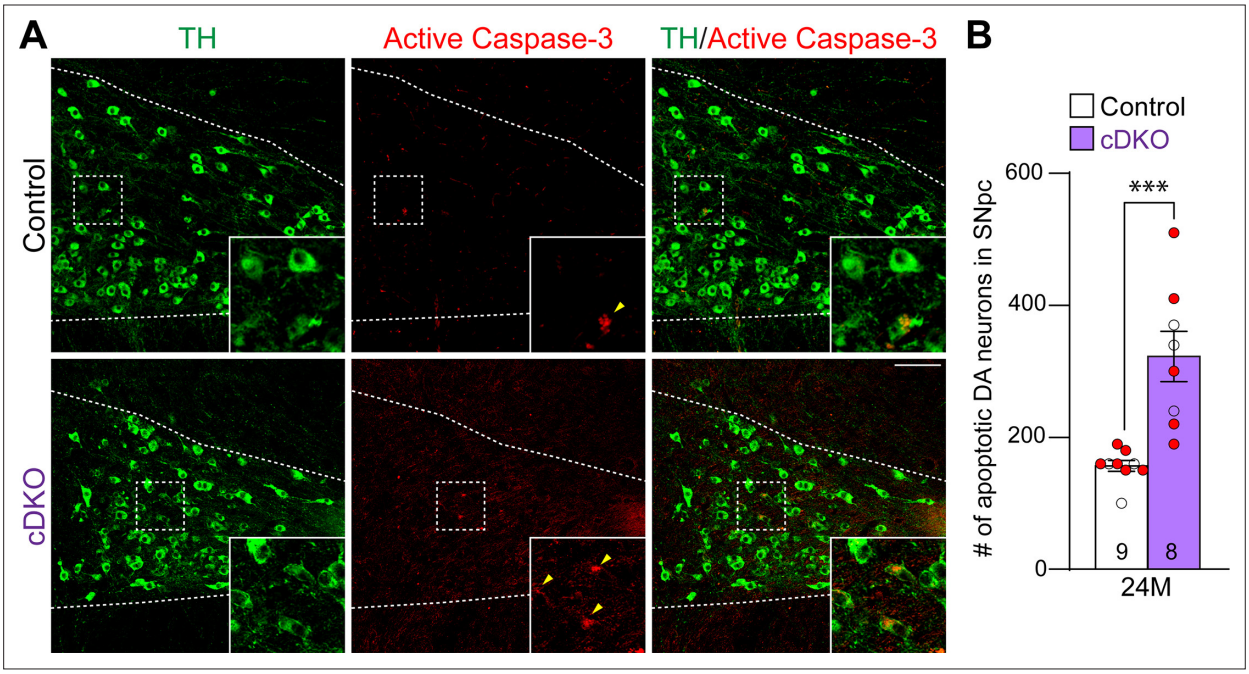

Figure 4. Increases in apoptotic dopaminergic (DA) neurons in the substantia nigra pars compacta (SNpc) of *Lrrk* conditional double knockout (cDKO) mice. (**A**) Representative images of TH and active Caspase-3 immunostaining show TH+ DA neurons (green) and active Caspase-3+ apoptotic cells (red) in the SNpc of *Lrrk* cDKO and control mice at the age of 24 months. (**B**) Quantification of active Caspase-3+/TH+ cells shows significant increases in apoptotic DA neurons in the SNpc of *Lrrk* cDKO mice (323 ± 38) at 24 months of age, relative to controls (157 ± 8, p=0.0004, Student's *t*-test). Raw quantification data are included in ***Figure 4—source data 1***. The number in the column indicates the number of mice used in the study. Red-filled and open circles represent data obtained from individual male and female mice, respectively. All data are expressed as mean ± SEM. ***p<0.001. Scale bar: 100 μm.

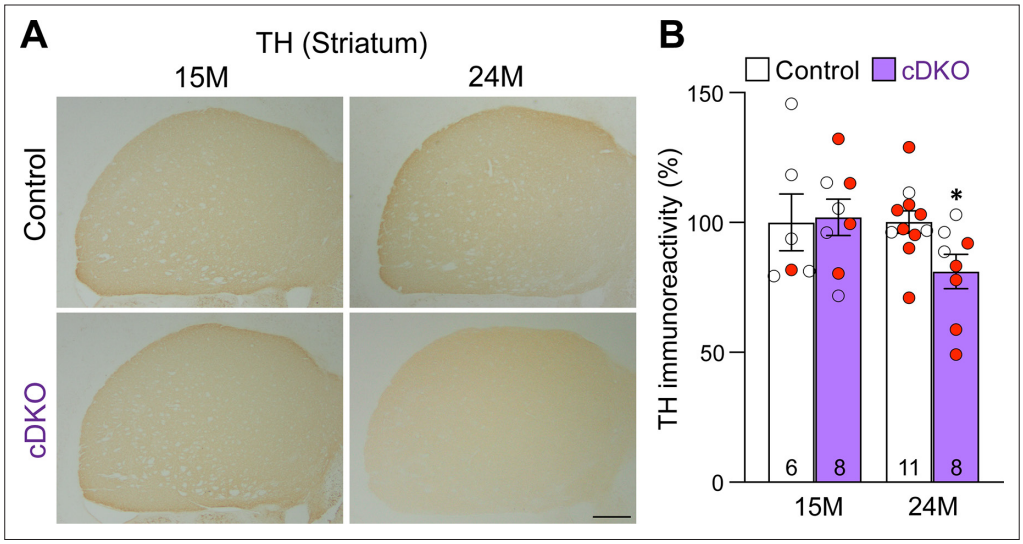

Figure 5. Age-dependent loss of TH+ dopaminergic (DA) terminals in the striatum of *Lrrk* conditional double knockout (cDKO) mice. (**A**) Representative TH immunostaining images in the striatum of *Lrrk* cDKO mice and littermate controls at the ages of 15 and 24 months. (**B**) Quantification of TH immunoreactivity in the striatum of *Lrrk* cDKO and control mice shows similar TH immunoreactivity at the age of 15 months (p=0.8766, Student's *t*-test), but there is a significant decrease in TH immunoreactivity in the striatum of *Lrrk* cDKO mice at 24 months of age (–19%, p=0.0215) compared to controls. The number in the column indicates the number of mice used in the study. Red-filled and open circles represent data obtained from individual male and female mice, respectively. All data are expressed as mean ± SEM. *p<0.05. Scale bar: 1 mm.

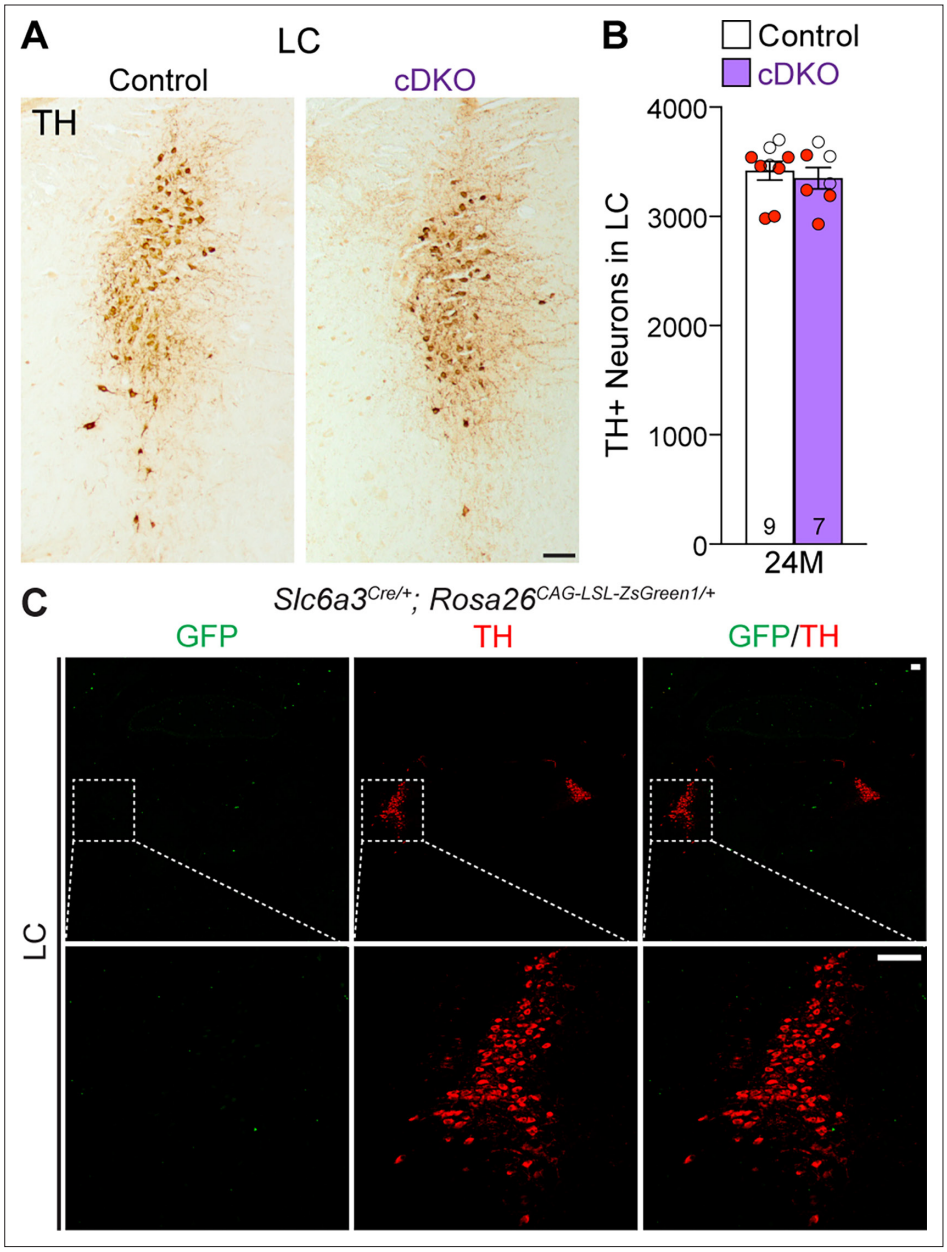

Figure 6. Normal number of TH+ noradrenergic neurons in the locus coeruleus (LC) of *Lrrk* conditional double knockout (cDKO) mice. (**A**) Representative images of TH+ noradrenergic neurons in the LC of *Lrrk* cDKO mice and littermate controls at 24 months of age. (**B**) Quantification of TH+ cells shows similar number of TH+ noradrenergic neurons in the LC of *Lrrk* cDKO mice (3350 ± 99) and controls (3418 ± 86, p=0.6110, Student's *t*-test). (**C**) Top: immunostaining of TH and GFP in the LC of *Slc6a3*$^{Cre/+}$; *Rosa26*$^{CAG\text{-}LSL\text{-}ZsGreen1/+}$ mice at 2 months of age. There is no GFP+ (green) cell in the LC, indicating that *Slc6a3-Cre* is not expressed in the LC. Bottom: higher power views of the boxed areas. The number in the column indicates the number of mice used in the study. Red-filled and open circles represent data obtained from individual male and female mice, respectively. All data are expressed as mean ± SEM. Scale bar: 100 μm.

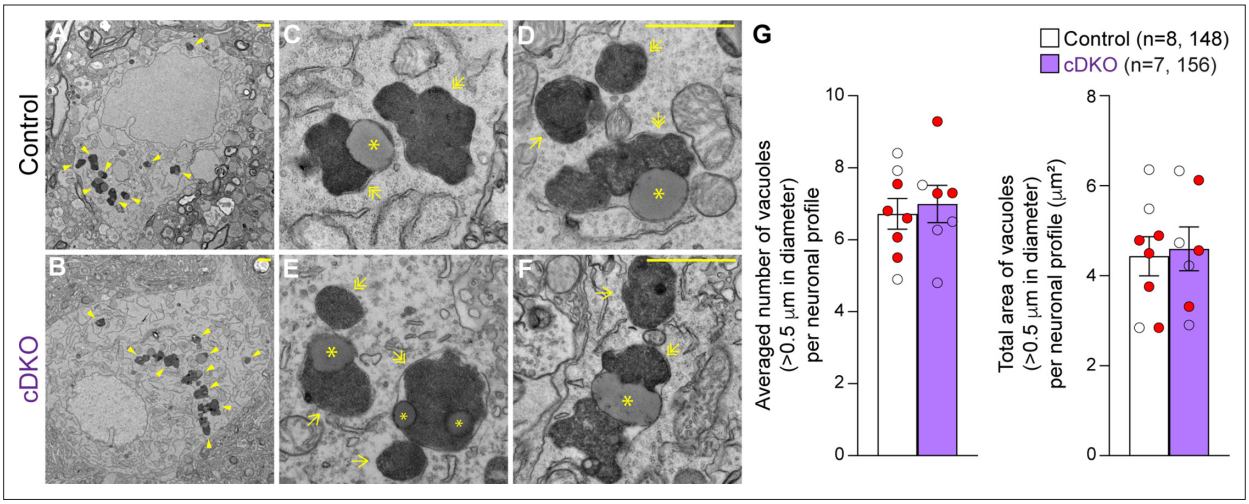

Figure 7. Unchanged number of electron-dense vacuoles in the substantia nigra pars compacta (SNpc) of *Lrrk* conditional double knockout (cDKO) mice. (**A, B**) Representative electron microscopy (EM) images showing electron-dense vacuoles (arrowheads) in SNpc neurons of cDKO mice and littermate controls at the age of 25 months. (**C–F**) Higher power views showing various electron-dense vacuoles, autolysosomes (single arrows), autophagosomes (double arrows), and lipid-containing vacuoles (asterisks) in SNpc neurons of littermate control (**C, D**) and cDKO (**E, F**) mice. (**G**) Left: the average number of electron-dense vacuoles (>0.5 μm in diameter) in the SNpc neuronal profiles per mouse is not significantly different between *Lrrk* cDKO mice and littermate controls at the age of 25 months (control: 6.72 ± 0.43; cDKO: 6.99 ± 0.52, p=0.6839, Student's *t*-test). Right: the total area of electron-dense vacuoles (>0.5 μm in diameter) in the SNpc neuronal profiles per mouse is similar between *Lrrk* cDKO and littermate controls (control: 4.43 ± 0.44 μm^2; cDKO: 4.60 ± 0.49 μm^2, p=0.8048). The value in parentheses indicates the number of mice (left) and neuron profiles (right) used in the quantification. Red-filled and open circles represent data obtained from individual male and female mice, respectively. All data are expressed as mean ± SEM. Scale bar: 1 μm.

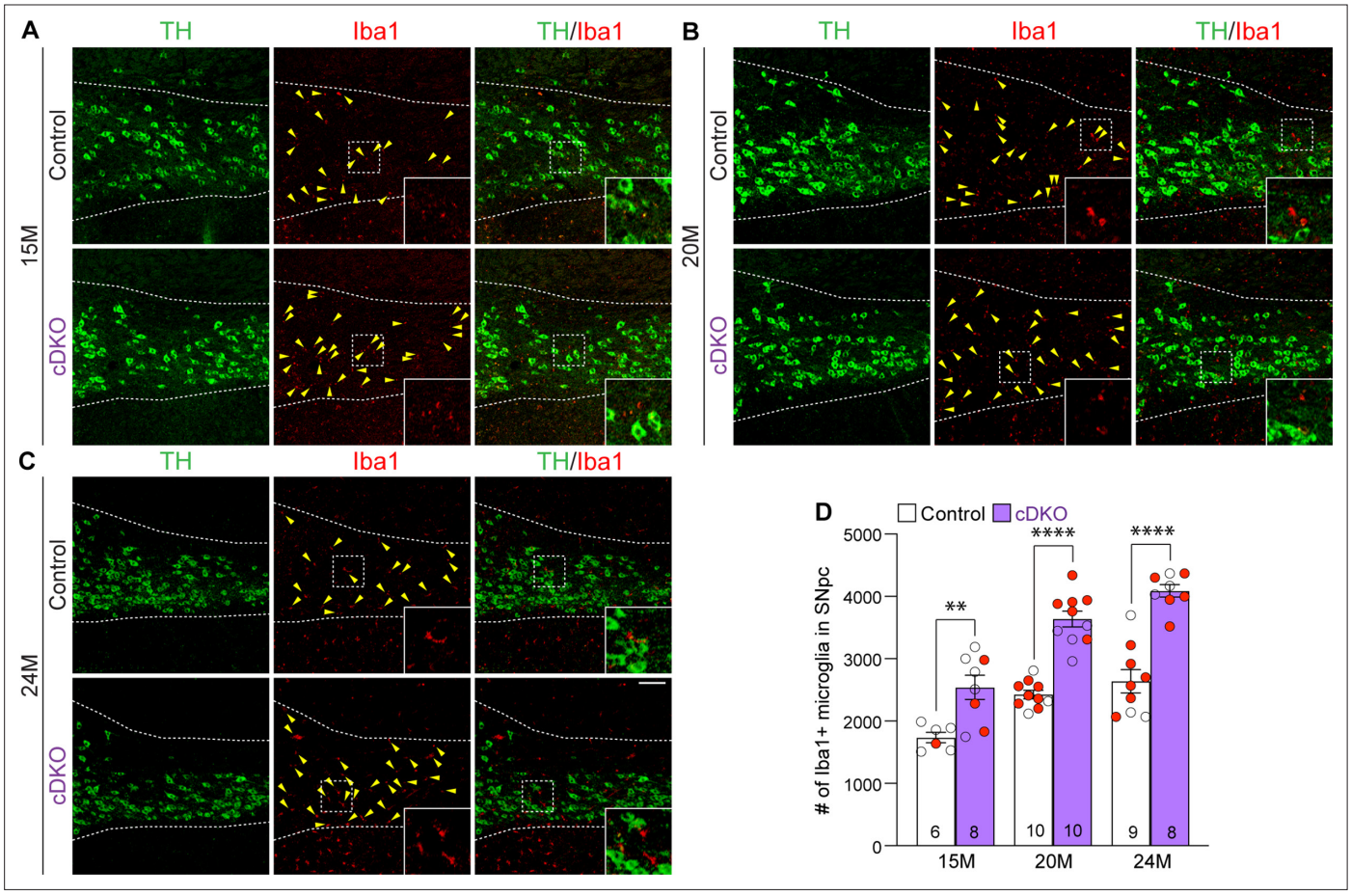

Figure 8. Elevated microgliosis in the substantia nigra pars compacta (SNpc) of *Lrrk* conditional double knockout (cDKO) mice. (**A–C**) Representative images of Iba1+ microglia (red, marked by yellow arrowheads) and TH+ dopaminergic neurons (green) in the SNpc of *Lrrk* DKO mice and controls at 15 (**A**), 20 (**B**), and 24 (**C**) months of age. (**D**) Quantification of Iba1+ microglia shows significant increases in the number of Iba1+ microglia in the SNpc of *Lrrk* cDKO mice compared to control mice at the ages of 15 months (control: 1737 ± 83, cDKO: 2541 ± 193; $F_{1,45}$ = 102.6, p<0.0001, p=0.0017, two-way ANOVA with Bonferroni's post hoc multiple comparisons), 20 months (control: 2426 ± 68, cDKO: 3639 ± 127, p<0.0001), and 24 months (control: 2640 ± 187, cDKO: 4089 ± 100, p<0.0001). Raw quantification data are included in ***Figure 8—source data 1***. The number in the column indicates the number of mice used in the study. Red-filled and open circles represent data obtained from individual male and female mice, respectively. All data are expressed as mean ± SEM. **p<0.01, ****p<0.0001. Scale bar: 100 μm.

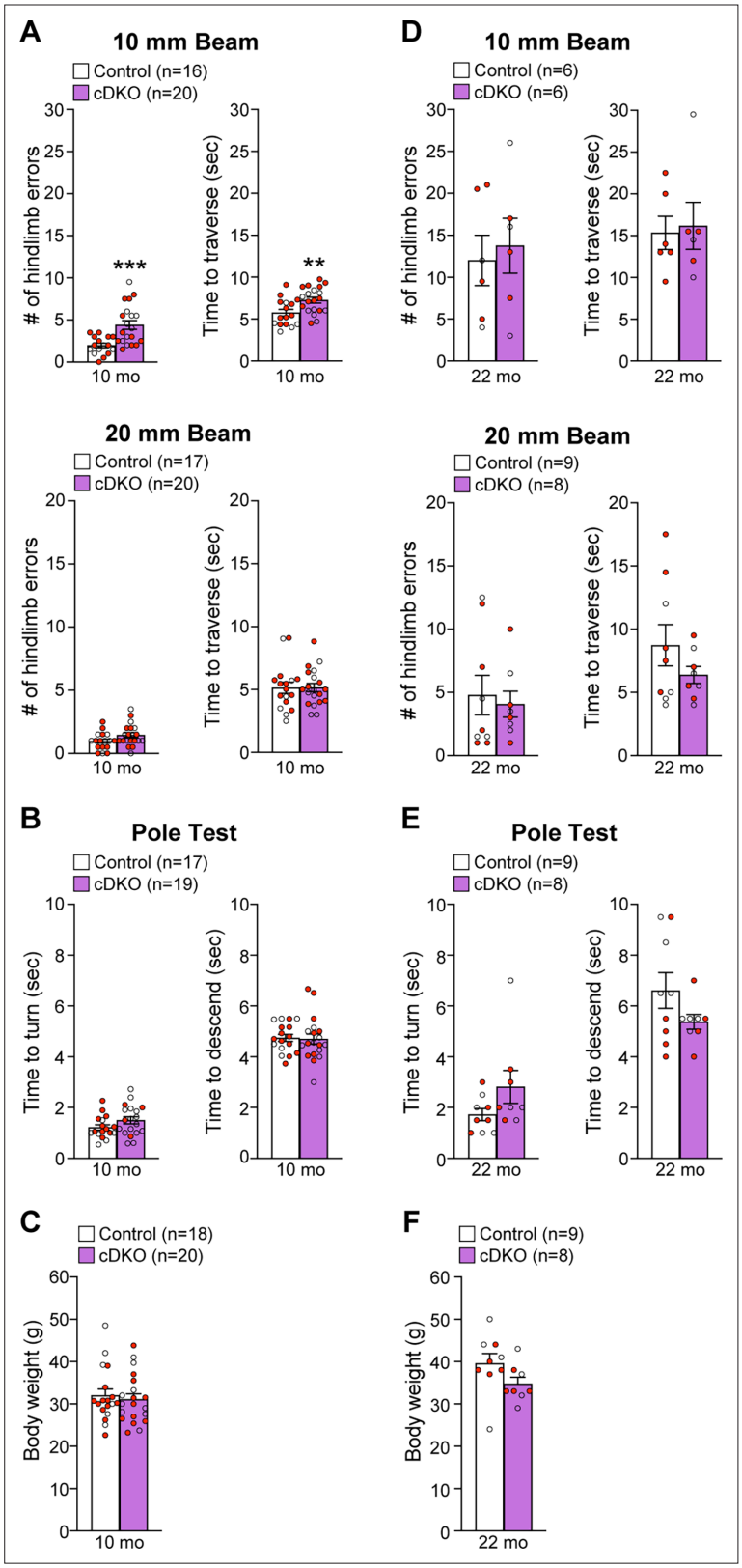

Figure 9. Impairment of motor coordination in *Lrrk* conditional double knockout (cDKO) mice. (**A**) In the 10 mm beam walk test, compared to control mice, *Lrrk* cDKO mice at 10 months of age exhibit markedly more hindlimb slips (control: 2.0 ± 0.3; cDKO: 4.4 ± 0.5; p=0.0005, Student's *t*-test) and longer traversal time (control: 5.8 ± 0.4; cDKO: 7.3 ± 0.3; p=0.0075). In the less challenging 20 mm beam walk test, there is no significant difference in

Figure 9 continued on next page

Figure 9 continued

the number of hindlimb slips (control: 1.0 ± 0.2; cDKO: 1.5 ± 0.2; p=0.0733) and traversal time (control: 5.1 ± 0.4; cDKO: 5.2 ± 0.3; p=0.9796) between *Lrrk* cDKO and control mice. (**B**) In the pole test, *Lrrk* cDKO and control mice at 10 months of age display similar turning time (control: 1.2 ± 0.1; cDKO: 1.5 ± 0.1; p=0.1219) and descending time (control: 4.7 ± 0.1; cDKO: 4.7 ± 0.2; p=0.8620). (**C**) *Lrrk* cDKO (31.1 ± 1.3) and control (32.0 ± 1.5; p=0.6410) mice at 10 months of age show similar body weight. (**D**) *Lrrk* cDKO mice and control mice at 22 months of age in the 10 mm beam walk test show similar hindlimb slips (control: 12.0 ± 3.0; cDKO: 13.8 ± 3.3; p=0.7022) and traversal time (control: 15.3 ± 2.0; cDKO: 16.2 ± 2.8; p=0.8139). In the 20 mm team walk test, there is also no difference in hindlimb slips (control: 4.8 ± 1.6; cDKO: 4.1 ± 1.0; p=0.7142) and traversal time (control: 8.7 ± 1.6; cDKO: 6.4 ± 0.7; p=0.2223) between *Lrrk* cDKO and control mice. (**E**) In the pole test, *Lrrk* cDKO mice at 22 months of age exhibit similar turning time (control: 1.7 ± 0.2; cDKO: 2.8 ± 0.7; p=0.1184) and descending time (control: 6.6 ± 0.7; cDKO: 5.4 ± 0.3; p=0.1413) compared to control mice. (**F**) *Lrrk* cDKO mice (34.8 ± 1.5) have similar body weight as control mice (39.6 ± 2.4; p=0.1194). The number in parentheses indicates the number of mice used in the study. Red-filled and open circles represent data obtained from individual male and female mice, respectively. All data are expressed as mean ± SEM. **p<0.01, ***p<0.001. Raw behavior data are included in ***Figure 9—source data 1***.